

Hydrogen Bonding Effects on the Surface Structure and Photoelectrochemical Properties of Nanostructured SnO₂ Electrodes Modified with Porphyrin and Fullerene Composites

Hiroshi Imahori,^{*,†,‡,§} Jia-Cheng Liu,[†] Hiroki Hotta,[‡] Aiko Kira,[†] Tomokazu Umeyama,[†] Yoshihiro Matano,[†] Guifeng Li,^{||} Shen Ye,^{*,||} Marja Isosomppi,[⊥] Nikolai V. Tkachenko,^{*,⊥} and Helge Lemmetyinen[⊥]

Department of Molecular Engineering, Graduate School of Engineering, Kyoto University, Nishikyo-ku, Kyoto 615-8510, Japan, PRESTO, Japan Science and Technology Agency (JST), Japan, Fukui Institute for Fundamental Chemistry, Kyoto University, 34-4, Takano-Nishihiraki-cho, Sakyo-ku, Kyoto 606-8103, Japan, Catalysis Research Center, Hokkaido University, Sapporo 001-0021, Japan, and Institute of Materials Chemistry, Tampere University of Technology, P. O. Box 541, FIN-33101 Tampere, Finland

Received: July 8, 2005

Hydrogen bonding effects on surface structure, photophysical properties, and photoelectrochemistry have been examined in a mixed film of porphyrin and fullerene composites with and without hydrogen bonding on indium tin oxide and nanostructured SnO₂ electrodes. The nanostructured SnO₂ electrodes modified with the mixed films of porphyrin and fullerene composites with hydrogen bonding exhibited efficient photocurrent generation compared to the reference systems without hydrogen bonding. Atomic force microscopy, infrared reflection absorption, and ultraviolet–visible absorption spectroscopies and time-resolved fluorescence lifetime and transient absorption spectroscopic measurements disclosed the relationship between the surface structure and photophysical and photoelectrochemical properties relating to the formation of hydrogen bonding between the porphyrins and/or the C₆₀ moieties in the films on the electrode surface. These results show that hydrogen bonding is a highly promising methodology for the fabrication of donor and acceptor composites on nanostructured semiconducting electrodes, which exhibit high photoelectrochemical properties.

Introduction

Noncovalent bonding such as hydrogen bonding, coordination bonding, electrostatic interaction, van der Waals interaction, and π – π interaction plays an important role in biological activities in nature. For instance, photosynthesis employs such weak interaction to arrange donor–acceptor (D–A) molecules in a protein matrix precisely, exhibiting a vectorial cascade of energy and electron-transfer processes.¹ Stimulated by this vision, the utilization of weak interaction has recently merited increasing attention as a sophisticated methodology to assemble supramolecular photosynthetic architectures.² A variety of noncovalently bonded D–A systems have been constructed in fluid media to mimic photoinduced energy and electron-transfer processes in photosynthesis.^{3–11}

Along this line, achieving efficient solar energy conversion at low cost is one of the most important technological challenges for the near future. During the past decade, organic solar cells have been discussed as a promising alternative to inorganic semiconductors for renewable energy production. Specifically, considerable attention has been drawn toward developing the dye-sensitized¹² and bulk heterojunction^{13–18} solar cells. The distinguishing characteristic of these cells is that excitations are generated upon light absorption, and within 100 fs charge

carriers are generated and simultaneously separated across the dye–semiconductor or donor–acceptor heterointerface. Typically, bulk heterojunction solar cells possess an interpenetrating network of donor (D) and acceptor (A) molecules in the blend film, revealing photoinduced charge separation and the transport of created charges to the electrodes. Thus, design and construction of electron- and hole-transporting, nanostructured highways in the D–A interpenetrating network are pivotal for enhancing both charge separation efficiency and charge carrier mobility. Supramolecular assembly of D–A molecules is a potential approach to create such a bulk heterojunction layer with a phase-separated, interpenetrating network involving nanostructured electron and hole highways. However, there have so far been few examples where a noncovalent bonding strategy has been employed in a mixed film of donor and acceptor to improve photocurrent generation efficiency in photoelectrochemical devices.^{15a,19,20}

Here, we report the first mixed films of porphyrin and fullerene with hydrogen bonding on tin oxide (SnO₂) as well as indium tin oxide (ITO) electrodes to reveal efficient photocurrent generation. The compounds used in this study are shown in Figure 1. A combination of porphyrin as a donor as well as a sensitizer with fullerene as an acceptor was chosen, because such a D–A system is known to exhibit a long-lived charge-separated state with a high quantum yield via photoinduced electron transfer.^{21,22} Given the fact that porphyrins tend to make a complex with fullerenes in a solid state due to the π – π interaction^{23–25} and the small reorganization energy of the porphyrin and fullerene system,^{21,22} we can expect fast photoinduced charge separation and slow charge recombination in the mixed film. More importantly, the resulting electron and

* To whom correspondence should be addressed. E-mail: (H.I.) imahori@scl.kyoto-u.ac.jp; (S.Y.) ye@cat.hokudai.ac.jp; (N.V.T.) nikolai.tkachenko@tut.fi.

[†] Kyoto University.

[‡] PRESTO, JST.

[§] Fukui Institute.

^{||} Hokkaido University.

[⊥] Tampere University of Technology.

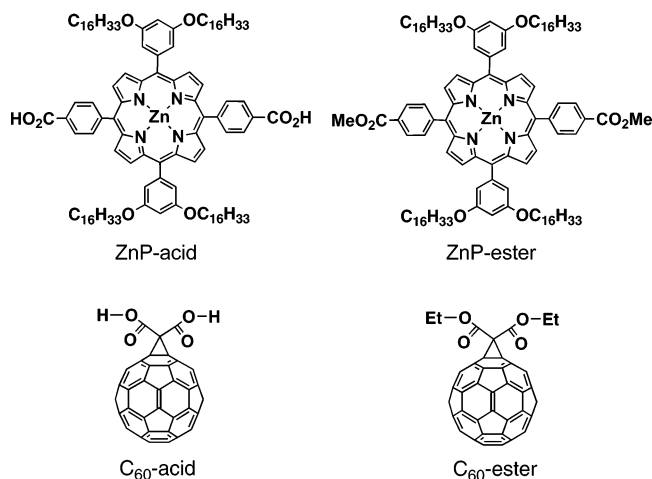


Figure 1. Porphyrin and fullerene derivatives used in this study.

hole pair must be separated through a tailored network of the acceptors and the donors, respectively, to suppress charge recombination. Such an electron- or hole-transporting highway would be constructed with the help of hydrogen bonding. To evaluate the hydrogen-bonding effect on the photoelectrochemical properties of the D–A systems, carboxyl and alkoxy carbonyl groups were introduced to porphyrin and C₆₀ to yield zinc porphyrin (ZnP) acid and ester as a donor (denoted as ZnP-acid and ZnP-ester) and C₆₀ acid and C₆₀ ester as an acceptor (denoted as C₆₀-acid and C₆₀-ester), respectively (Figure 1).

Experimental Section

General Methods. Melting points were recorded on a Yanagimoto micromelting point apparatus and not corrected. ¹H NMR spectra were measured on a JEOL EX-400 spectrometer. Matrix-assisted laser desorption/ionization (MALDI) time-of-flight mass spectra (TOF) were measured on a Kratos compact MALDI I (Shimadzu). UV-visible absorption spectra were obtained on a Perkin-Elmer Lambda 900UV/vis/near-IR spectrometer.

Infrared reflection absorption (IRRA) spectra were recorded by a Bio-Rad FTS 575C FT-IR spectrometer equipped with a liquid-N₂-cooled MCT detector and a Harrick Reflector grazing angle reflectance unit.²⁶ The samples for IRRA observation were prepared by direct deposition of these functional molecules on a slide glass (2 × 2 cm²) covered by a 200 nm thick gold film for IRRA observation, by spin-coating method. The IRRA spectrum of a bare gold film was used as the reference. The spectral resolution used was 4 cm⁻¹.

Atomic force microscopy (AFM) measurements were carried out using a Digital Nanoscope III in the tapping mode. Steady-state fluorescence spectra were measured on a Fluorolog 3 spectrofluorimeter (ISA Inc.) equipped with a cooled IR-sensitive photomultiplier (R2658). All solvents and chemicals were of reagent grade quality and were purchased commercially and used without further purification unless otherwise noted. Tetrabutylammonium hexafluorophosphate used as a supporting electrolyte for the electrochemical measurements was obtained from Fluka and recrystallized from methanol. Thin-layer chromatography and flash column chromatography were performed with Alt. 5554 DCAIulofien Kieselgel 60 F₂₅₄ (Merck) and silica gel 60N (Kanto Chemicals), respectively. ITO electrodes (190–200 nm ITO on transparent glass slides) were commercially available from Tokyo Sanyo Sinku. The roughness factor (*R* = 1.3) was estimated by AFM measurement with tapping mode.

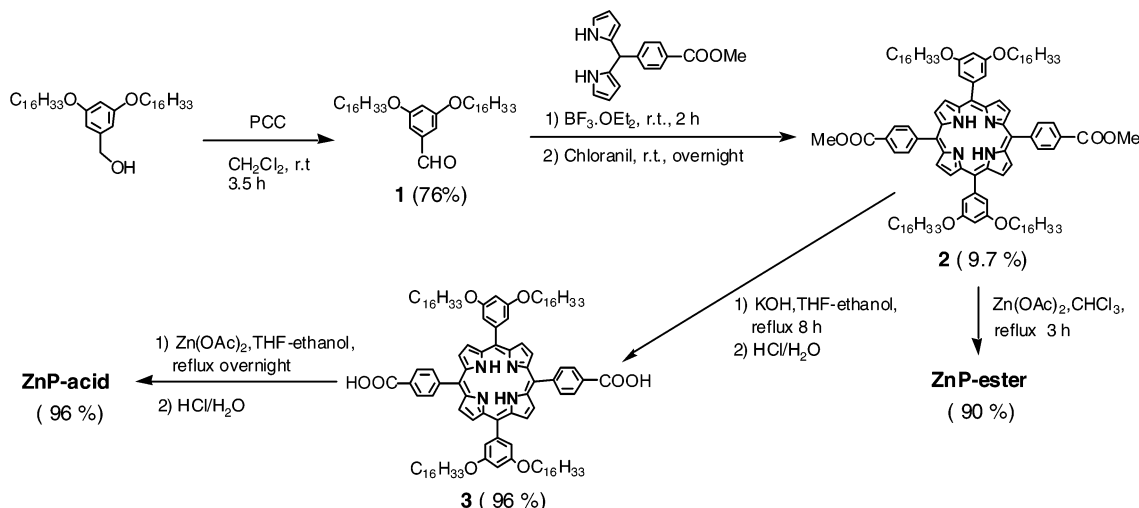
Synthesis and Characterization. *Compound 1.* To a solution of 3,5-dihexadecyloxybenzyl alcohol²⁷ (5.8 g, 9.85 mmol) in dried dichloromethane (90 mL) was added a suspension of PCC (5.5 g) in dried dichloromethane (20 mL) with stirring for 3.5 h at room temperature. The resulting mixture was filtered, and the residue was washed several times with dichloromethane. The filtrate was collected, and the solvent was removed under reduced pressure. Flash column chromatography on silica gel (hexane/ethyl acetate = 96:4) afforded **1** as a white solid (4.4 g, 7.5 mmol, 76%). Mp 54–55 °C; IR (KBr) 3100, 2953 2917, 2851, 1710, 1683, 1596, 1472, 1392, 1325, 1319, 1180, 1059, 943, 848, 834, 734, 717, 675 cm⁻¹; ¹H NMR (400 MHz, CDCl₃) δ 0.88 (t, *J* = 6.8 Hz, 6H), 1.26 (m, 52H), 1.79 (m, 4H), 3.98 (t, *J* = 6.4 Hz, 4H), 6.70 (t, *J* = 2.0 Hz, 1H), 6.98 (d, *J* = 2.0 Hz, 2H), 9.89 (s, 1H); MALDI-TOFMS (positive mode) *m/z* 588 (M + H⁺); Anal. Calcd for C₃₉H₇₀O₃: C, 79.80; H, 12.02. Found: C, 79.59; H, 12.05.

Compound 2. A solution of 5-(4-methoxycarbonylphenyl)-dipyrrromethane²⁸ (1.40 g, 5 mmol) and **1** (2.93 g, 5 mmol) in chloroform (500 mL) with stirring at room temperature under nitrogen was treated with boron trifluoride diethyl etherate (0.64 mL, 5.06 mmol).²⁸ After 2 h, *p*-chloranil (1.86 g, 7.6 mmol) was added, and the reaction mixture was stirred overnight. Triethylamine (2.1 mL, 15.2 mmol) was added, and the resulting mixture was concentrated. Subsequent flash column chromatography on silica gel (hexane/toluene = 3:1→1:3) yielded **2** as a reddish purple solid (0.41 g, 0.24 mmol, 9.7%). Mp 127–128 °C; IR (KBr) 3315, 2921, 2852, 1725, 1590, 1471, 1430, 1394, 1354, 1311, 1276, 1256, 1155, 1109, 1100, 1054, 1022, 974, 927, 848, 799, 778, 732, 720, 633 cm⁻¹; ¹H NMR (400 MHz, CDCl₃) δ 2.83 (br s, 2H), 0.85 (t, *J* = 6.8 Hz, 12H), 1.22 (m, 104 H), 1.85 (m, 8H), 4.11 (t, *J* = 6.4 Hz, 8H), 4.12 (s, 6H), 6.88 (t, *J* = 2.0 Hz, 2H), 7.36 (d, *J* = 2.0 Hz, 4H), 8.30 (d, *J* = 8.4 Hz, 4H), 8.44 (d, *J* = 8.4 Hz, 4 H), 8.77 (d, *J* = 4.8 Hz, β-H, 4H), 8.98 (d, *J* = 4.8 Hz, β-H, 4H); MALDI-TOFMS (positive mode) *m/z* 1693 (M + H⁺).

Compound 3. A mixture of **2** (0.17 g, 0.1 mmol) in 100 mL of tetrahydrofuran (THF)–ethanol (1:1) and potassium hydroxide (0.513 g) in water (5 mL) was refluxed for 8 h. After cooling and the removal of solvent, the residue was diluted with water (100 mL) and desired porphyrin dipotassium salt was filtered. Acidification (pH 2) of an aqueous suspension of the porphyrin dipotassium salt with concentrated hydrochloric acid and subsequent filtration gave **3** as a reddish purple powder (0.16 g, 0.1 mmol, 96%). Mp >300 °C; IR (KBr) 3318, 3090, 2921, 2852, 2533, 1690, 1599, 1589, 1541 1467, 1430, 1383, 1354, 1310, 1292, 1250, 1162 1129, 1057, 1020, 974, 928, 849, 830, 799, 778, 724, 711, 699 cm⁻¹; ¹H NMR (400 MHz, CDCl₃/DMSO-*d*₆ = 3:2) δ 2.91 (br s, 2H), 0.83 (t, *J* = 6.0 Hz, 12H), 1.18 (m, 104H), 1.81 (m, 8H), 4.10 (t, *J* = 6.0 Hz, 8H), 6.86 (t, *J* = 2.0 Hz, 2H), 7.31 (d, *J* = 2.0 Hz, 4H), 8.20 (d, *J* = 8.0 Hz, 4 H), 8.41(d, *J* = 8.0 Hz, 4 H), 8.83 (d, *J* = 4.8 Hz, β-H, 4H), 8.95 (d, *J* = 4.8 Hz, β-H, 4H); MALDI-TOFMS (positive mode) *m/z* 1665 (M + H⁺).

ZnP-Acid. To the solution of **3** (0.30 g, 0.18 mmol) in 300 mL of THF–ethanol (1:1) was added a solution of zinc acetate dihydrate (0.20 g, 0.91 mmol) in methanol (4 mL). The reaction mixture was refluxed overnight. After cooling and following removal of solvent, the residue was treated with 150 mL of 1 M HCl aqueous solution and 500 mL of CHCl₃ with stirring overnight. The CHCl₃ layer was collected, washed with water several times, dried over anhydrous Na₂SO₄, and concentrated in vacuo. The resulting solid was purified by chromatography on silica gel eluting with CH₂Cl₂/THF (95:5) to yield ZnP-acid

SCHEME 1



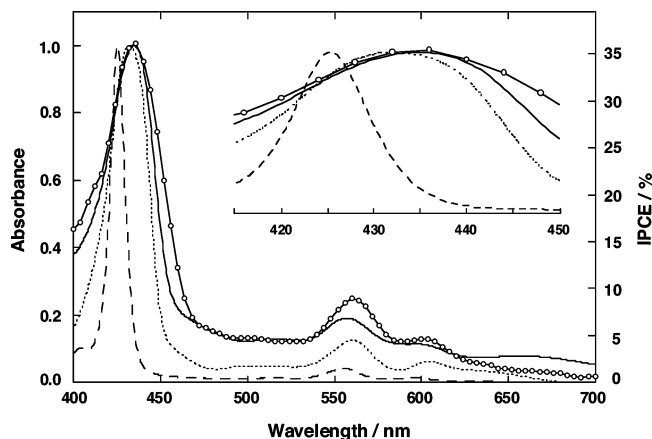


Figure 2. UV-visible absorption spectra of a mixed film of ZnP-acid and C₆₀-acid ((ZnP-acid + C₆₀-acid)/SnO₂/ITO, solid line), a film of ZnP-acid (ZnP-acid/SnO₂/ITO, dotted line), an equimolar THF solution of ZnP-acid and C₆₀-acid (ZnP-acid + C₆₀-acid, dashed line), and action spectrum of (ZnP-acid + C₆₀-acid)/SnO₂/ITO system (solid line with open circles): input power, 85 μW cm⁻² (λ_{ex} = 435 nm); applied potential, 0.15 V vs SCE; 0.5 M LiI and 0.01 M I₂ in acetonitrile. The spectra were normalized at the Soret band for comparison. Expanded spectra in the Soret band region are shown as an inset. The modified SnO₂/ITO electrodes were prepared by immersing SnO₂/ITO electrodes into an equimolar THF solution (1.5 mM) of ZnP-acid and C₆₀-acid.

benzyl alcohol was oxidized using PCC to yield benzaldehyde **1**.²⁷ Porphyrin **2** was synthesized by the condensation of 5-(4-methoxycarbonylphenyl)dipyromethane with **1** in the presence of BF₃·OEt₂.²⁸ Porphyrin diester **2** was hydrolyzed to give porphyrin dicarboxylic acid **3**. ZnP-acid was obtained by treatment of **3** with Zn(OAc)₂. ZnP-ester was prepared from **2** in the same manner. C₆₀-ester³⁰ and C₆₀-acid³⁰ were synthesized by following previously reported procedures.

Characterization and Surface Structure of SnO₂/ITO and ITO Electrodes Modified with Porphyrin and Fullerene Composites. We have successfully observed enhanced photocurrent generation in ITO electrode modified with the mixed film of porphyrin and hydrogen-bonded C₆₀ derivative relative to the reference system without hydrogen bonding.^{19b} To improve the photovoltaic properties of the previous system, hydrogen-bonding strategy has been also applied to the porphyrin moiety in addition to the C₆₀ moiety (Figure 1). More importantly, ITO electrode is replaced by SnO₂/ITO electrode to suppress charge recombination. Once the separated electron is injected into the conduction band (CB) of SnO₂, there would be less chance to recombine the electron in the conduction band and the hole in porphyrin radical cation or electron carrier in the electrolyte solution, leading to the remarkable improvement of photocurrent generation efficiency.

SnO₂/ITO electrodes were immersed into an equimolar THF solution (1.5 mM) of porphyrin (ZnP-acid, ZnP-ester) and/or fullerene (C₆₀-acid, C₆₀-ester) to give modified SnO₂/ITO electrodes. Figure 2 shows absorption spectra of a mixed film of ZnP-acid and C₆₀-acid (denoted as (ZnP-acid + C₆₀-acid)/SnO₂/ITO), a film of ZnP-acid (denoted as ZnP-acid/SnO₂/ITO), and the equimolar THF solution of ZnP-acid and C₆₀-acid (denoted as ZnP-acid + C₆₀-acid). The Soret bands of (ZnP-acid + C₆₀-acid)/SnO₂/ITO and ZnP-acid/SnO₂/ITO are broadened and red-shifted relative to that of ZnP-acid + C₆₀-acid in THF due to the interaction between the porphyrins. In addition, the broad long wavelength absorption of (ZnP-acid + C₆₀-acid)/SnO₂/ITO in the 600–700 nm regions is diagnostic of the charge-transfer absorption band due to the π-complex formed

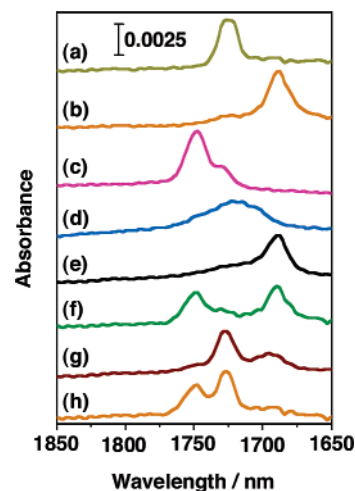


Figure 3. IRRA spectra in the C=O stretching region (1650–1850 cm⁻¹) for the thin films of porphyrin and/or fullerene spin-coated on gold surface as (a) ZnP-ester, (b) ZnP-acid, (c) C₆₀-ester, (d) C₆₀-acid, (e) ZnP-acid + C₆₀-acid, (f) ZnP-acid + C₆₀-ester, (g) ZnP-ester + C₆₀-acid, and (h) ZnP-ester + C₆₀-ester. IR intensities for mixed films were normalized to the same concentration as those for single-component films.

between the porphyrin and the C₆₀.^{20,25} Similar spectral behavior was observed for the modified SnO₂/ITO electrodes prepared by the spin-coating method.

Figure 3 shows IRRA spectra in the C=O stretching region (1650–1850 cm⁻¹) for the thin films of porphyrin and/or fullerene spin-coated on gold surface as (a) ZnP-ester, (b) ZnP-acid, (c) C₆₀-ester, (d) C₆₀-acid, (e) ZnP-acid + C₆₀-acid, (f) ZnP-acid + C₆₀-ester, (g) ZnP-ester + C₆₀-acid, and (h) ZnP-ester + C₆₀-ester. Detailed peak information is summarized in Table 1. As shown in Figure 3a, ZnP-ester gives an IR peak at 1725 cm⁻¹ which can be assigned to the free C=O stretching mode of the ester moiety. In contrast with ZnP-ester, ZnP-acid shows an IR absorption peak from C=O stretching at lower wavenumber (1688 cm⁻¹, Figure 3b). Normally, it is known that the peak from C=O stretching mode shifts to lower frequency region when the hydrogen bonding is formed between carbonyl group and a hydrogen-bonding donor.^{31–35} Thus, the red shift in peak position of the C=O stretching can be attributed to the formation of intermolecular hydrogen bonding between ZnP-acid molecules, possibly dimer or some higher aggregates.

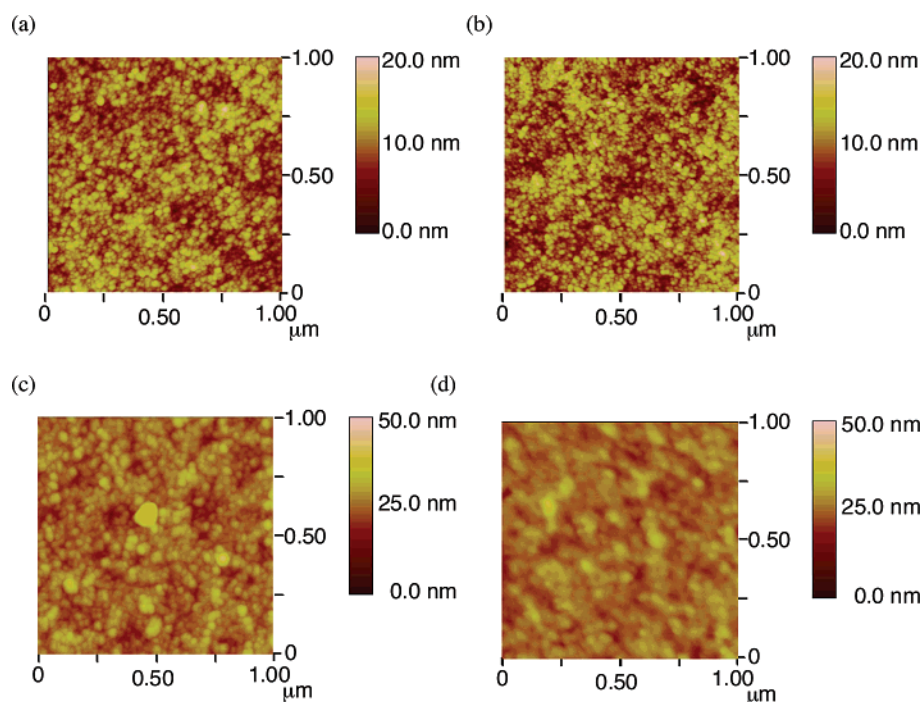
Furthermore, C₆₀-ester shows an IR peak at 1748 cm⁻¹ with a shoulder at 1729 cm⁻¹ (Figure 3c), while C₆₀-acid gives a broad IR peak around 1720 cm⁻¹ (Figure 3d), suggesting the formation of hydrogen bonding between C₆₀-acid molecules. The reason for the relatively broad shape of the IRRA spectrum of C₆₀-acid is not clear at this stage and may be related to the un-uniform aggregates of C₆₀-acid on the substrate.

On the other hand, useful structural information about the hydrogen-bonding interaction between different types of molecules can be obtained from the IRRA spectra of mixed films of porphyrin and fullerene composites. As shown in Figure 3e,f, an IR peak at 1688 cm⁻¹ was clearly observed for ZnP-acid mixed with C₆₀-acid or C₆₀-ester. It is unlikely that the hydrogen-bonding interaction between ZnP-acid and C₆₀-acid or C₆₀-ester is strong since these IR spectra look like a superimposition of IR spectra of two single respective components. For example, the C=O stretching mode of C₆₀-ester in the equimolar mixture film with ZnP-acid shows nearly the same feature as that of a single C₆₀-ester component and obvious changes in peak position and intensity were not observed (Figure 3f), indicating that interaction between ZnP-acid and C₆₀-ester species is very

TABLE 1: IRRA Frequencies, IPCE Values, and Fluorescence Lifetimes

system	IRRA freq/cm ⁻¹	IPCE (dipping method) value ^a /%	IPCE (spin-coating method) value ^b /%	fluorescence lifetime ^c /ps
ZnP-acid + C ₆₀ -acid	1688, 1720	36	18	<i>d</i>
ZnP-acid + C ₆₀ -ester	1689, 1749	28	8.2	<i>d</i>
ZnP-ester + C ₆₀ -acid	1694, 1727	15	7.1	40
ZnP-ester + C ₆₀ -ester	1726, 1749	7	2.6	62
ZnP-acid	1688	26	3.5	<i>d</i>
ZnP-ester	1725	6	1.2	380
C ₆₀ -acid	1720	<i>e</i>	<i>e</i>	<i>e</i>
C ₆₀ -ester	1748, 1729	<i>e</i>	<i>e</i>	<i>e</i>

^a Input power, 85 μW cm⁻² (λ_{ex} = 435 nm); absorbance, 1.00 ± 0.05 at excitation wavelength; thickness of SnO₂ layer, 1.1 μm; applied potential, 0.15 V vs SCE. ^b Input power, 92 μW cm⁻² (λ_{ex} = 435 nm); absorbance, 0.25 ± 0.03 at excitation wavelength; thickness of SnO₂ layer, 0.4 μm; applied potential, 0.15 V vs SCE. ^c The samples were prepared by dipping method. The fluorescence decays were measured by time-correlated single photon counting method (λ_{ex} = 590 nm); the monitoring wavelength was at 660 nm. ^d The decay was too fast to give the fluorescence lifetime accurately. ^e Not measured.

**Figure 4.** AFM images of (a) ZnP-acid/SnO₂/ITO, (b) ZnP-ester/SnO₂/ITO, (c) C₆₀-acid/SnO₂/ITO, and (d) C₆₀-ester/SnO₂/ITO electrodes.

limited. At the same time, we still expect that a small part of ZnP-acid molecules may form hydrogen bonding with C₆₀-acid molecules, although the hydrogen bonding interaction between the same types of molecules (i.e., ZnP-acid and ZnP-acid, C₆₀-acid and C₆₀-acid) seemed to be stronger. It is noteworthy that an equimolar mixture of ZnP-ester and C₆₀-acid shows slightly different behavior (Figure 1g), where the peak position of C=O stretching from C₆₀-acid in the mixture film was narrower and was shifted to 1694 cm⁻¹ in comparison with that of the single C₆₀-acid component, suggesting that the hydrogen bonding in C₆₀-acid was intensified in the mixture with ZnP-ester (vide infra). As expected, no change was observed in the mixture of ZnP-ester molecules and C₆₀-ester molecules (Figure 3h) since there is no hydrogen-bonding donor.

As demonstrated above, the formation of hydrogen bonding was confirmed in the mixed film of ZnP-acid + C₆₀-acid, ZnP-acid + C₆₀-ester as well as ZnP-ester + C₆₀-acid but not in ZnP-ester + C₆₀-ester. The hydrogen-bonding interaction between the ZnP-acid molecules or C₆₀-acid molecules seems to be more important than that between different types of molecules.

AFM measurements were performed for the SnO₂/ITO electrodes modified with the compounds by spin-coating method

(Figures 4 and 5). The images of ZnP-acid/SnO₂/ITO (Figure 4a) and ZnP-ester/SnO₂/ITO (Figure 4b) are similar to that of bare SnO₂/ITO, which exhibit arrays of spherical particles with 20 nm size. In contrast, the images of C₆₀-acid/SnO₂/ITO (Figure 4c) and C₆₀-ester/SnO₂/ITO (Figure 4d) show arrays of spherical particles with 30–40 nm size, which is larger than that of ZnP-acid/SnO₂/ITO and ZnP-ester/SnO₂/ITO. These results together with the IRRA spectra suggest that the C₆₀ molecules are more aggregative than the porphyrins (vide supra). The AFM images of the porphyrin and C₆₀ mixed system are quite different from those of either the porphyrin or the C₆₀ system. The AFM images of (ZnP-acid + C₆₀-acid)/SnO₂/ITO (Figure 5a), (ZnP-acid + C₆₀-ester)/SnO₂/ITO (Figure 5b), and (ZnP-ester + C₆₀-acid)/SnO₂/ITO (Figure 5c) are much smoother than those of (ZnP-ester + C₆₀-ester)/SnO₂/ITO (Figure 5d) as well as of ZnP-acid/SnO₂/ITO, ZnP-ester/SnO₂/ITO, C₆₀-acid/SnO₂/ITO, and C₆₀-ester/SnO₂/ITO (see Supporting Information, S1). A similar trend was observed for the AFM images on ITO and mica surfaces. These results demonstrate that both the intermolecular interaction between the porphyrin and the C₆₀ and the hydrogen bonding from either the porphyrin or the C₆₀ moieties are required for the smooth morphology on the surface in which the porphyrin and the C₆₀ molecules would be self-assembled

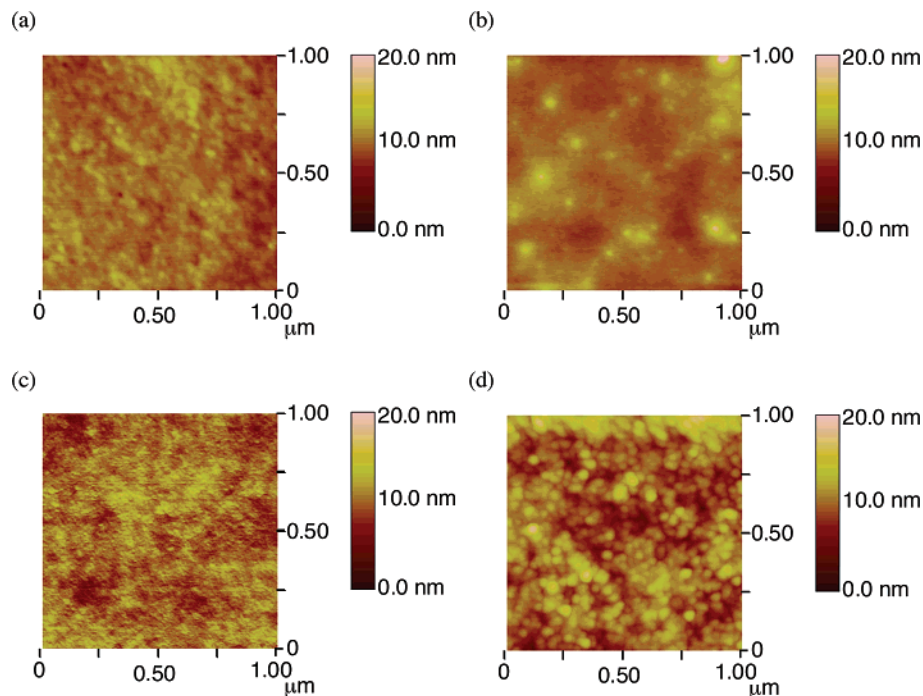


Figure 5. AFM images of (a) (ZnP-acid + C₆₀-acid)/SnO₂/ITO, (b) (ZnP-acid + C₆₀-ester)/SnO₂/ITO, (c) (ZnP-ester + C₆₀-acid)/SnO₂/ITO, and (d) (ZnP-ester + C₆₀-ester)/SnO₂/ITO ([ZnP]/[C₆₀] = 1:1) electrodes.

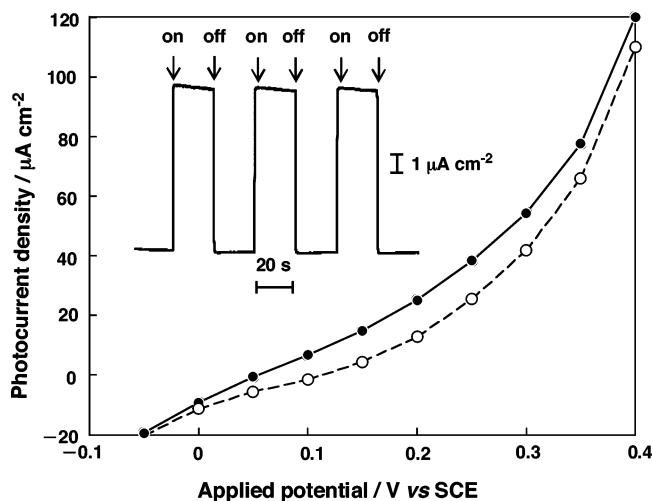


Figure 6. Photocurrent vs applied potential curves of (ZnP-acid + C₆₀-acid)/SnO₂/ITO system. The dark currents are shown as a dashed line with open circles. Experimental conditions were as follows: excitation power, 85 μW cm⁻² (λ_{ex} = 435 nm); absorbance, 1.00 at excitation wavelength; thickness of SnO₂ layer, 1.1 μm; 0.5 M LiI and 0.01 M I₂ in acetonitrile. The photoelectrochemical response at applied potential of 0.15 V vs SCE is shown as an inset.

with a phase-separated, interpenetrating network involving hydrogen-bonded electron and/or hole-transporting nanostructures (vide infra).

Photoelectrochemical Properties of SnO₂/ITO and ITO Electrodes Modified with Porphyrin and Fullerene Composites. Photoelectrochemical measurements were performed in a nitrogen-saturated acetonitrile solution containing 0.5 M LiI and 0.01 M I₂ using the modified SnO₂/ITO as the working electrode, a platinum counter electrode, and a I⁻/I₃⁻ reference electrode. For instance, a stable anodic photocurrent from the electrolyte to (ZnP-acid + C₆₀-acid)/SnO₂/ITO electrode, prepared by the dipping method, appeared immediately upon irradiation of the modified SnO₂/ITO electrode (Figure 6). The photocurrent fell down instantly when the illumination was cut

off. The intensity of the photocurrent was maintained almost constant during the irradiation at least 1 h. The anodic photocurrent increases with increasing positive bias to the ITO electrode from -0.05 to +0.4 V vs SCE, as shown in Figure 6. The agreement of the action spectrum with the absorption spectrum of (ZnP-acid + C₆₀-acid)/SnO₂/ITO, which is largely similar to that of ZnP-acid/SnO₂/ITO (Figure 2), demonstrates that the direction of the electron flow is from the electrolyte to the ITO via the excited singlet state of the porphyrin moiety (vide infra). Similar photoelectrochemical behavior was observed for (ZnP-acid + C₆₀-ester)/SnO₂/ITO, (ZnP-ester + C₆₀-acid)/SnO₂/ITO, (ZnP-ester + C₆₀-ester)/SnO₂/ITO, ZnP-acid/SnO₂/ITO, and ZnP-ester/SnO₂/ITO systems.

The IPCE (incident photon-to-photocurrent efficiency) values were compared for (ZnP-acid + C₆₀-acid)/SnO₂/ITO, (ZnP-acid + C₆₀-ester)/SnO₂/ITO, (ZnP-ester + C₆₀-acid)/SnO₂/ITO, (ZnP-ester + C₆₀-ester)/SnO₂/ITO, ZnP-acid/SnO₂/ITO, and ZnP-ester/SnO₂/ITO systems under the same conditions (applied potential, 0.15 V vs SCE; λ_{ex} = 435 nm). The excitation wavelength at the Soret band guarantees the selective excitation of the porphyrin rather than that of C₆₀ moiety. The IPCE values obtained by the dipping method are in the order of (ZnP-acid + C₆₀-acid)/SnO₂/ITO (36%) > (ZnP-acid + C₆₀-ester)/SnO₂/ITO (28%) > ZnP-acid/SnO₂/ITO (26%) > (ZnP-ester + C₆₀-acid)/SnO₂/ITO (15%) > (ZnP-ester + C₆₀-ester)/SnO₂/ITO (7%) > ZnP-ester/SnO₂/ITO (6%) systems (Table 1). The IPCE values are larger by 1–2 orders of magnitudes than those of a similar porphyrin-hydrogen-bonded C₆₀ system on ITO electrode.^{19b} The IPCE values from ZnP-acid systems are much larger than those from ZnP-ester systems. This difference may result from direct adsorption of ZnP-acid onto the SnO₂ surface, where an electron is directly injected into the conduction band of the SnO₂ surface from the excited singlet state of the porphyrin to generate photocurrent.^{36,37} In both the porphyrin carboxylic acid system and the porphyrin ester system, IPCE values increase significantly when C₆₀ acid rather than C₆₀ ester is employed. This suggests that not only the direct electron injection takes place but also a competitive electron transfer

occurs from the porphyrin excited singlet state to C₆₀-acid, followed by the electron injection from the reduced C₆₀ to the conduction band of the SnO₂ surface (vide infra). Besides, electron and hole relay may occur in the arrays of hydrogen-bonded C₆₀-acid and ZnP-acid, respectively, as indicated from the dominant hydrogen-bonding interaction between the identical ZnP-acid molecules or C₆₀-acid molecules rather than between different types of molecules (vide supra). It is noteworthy that the IPCE value is improved in the mixed system with hydrogen bonding as compared to the reference system. Although the largest IPCE value (36%) is achieved in the (ZnP-acid + C₆₀-acid)/SnO₂/ITO system,^{38,39} the hydrogen-bonding effect on photocurrent generation is not prominent in comparison with (ZnP-acid + C₆₀-ester)/SnO₂/ITO and ZnP-acid/SnO₂/ITO systems. It may be originated from the dipping method in which ZnP-acid and C₆₀-acid tend to adsorb onto the SnO₂ surface rather than hydrogen bonding to each other. To differentiate the two competitive processes, the fabrication of these molecules on the SnO₂/ITO electrodes were carried out by using spin-coating method, which reduces the possibility of adsorbing ZnP-acid and C₆₀-acid onto the SnO₂/ITO electrodes significantly. Although the IPCE values obtained by the spin-coating method are smaller than those obtained by the dipping method, the former trend for the IPCE values is unambiguous: (ZnP-acid + C₆₀-acid)/SnO₂/ITO (18%) > (ZnP-acid + C₆₀-ester)/SnO₂/ITO (8.2%) > (ZnP-ester + C₆₀-acid)/SnO₂/ITO (7.1%) > ZnP-acid/SnO₂/ITO (3.5%) > (ZnP-ester + C₆₀-ester)/SnO₂/ITO (2.6%) > ZnP-ester/SnO₂/ITO (1.2%) systems. The trend for the IPCE values is in good agreement with the results on the IRRA spectra and the AFM measurements. For instance, the IPCE value (18%) of the (ZnP-acid + C₆₀-acid)/SnO₂/ITO system is much larger than those of (ZnP-acid + C₆₀-ester)/SnO₂/ITO (8.2%) and ZnP-acid/SnO₂/ITO (3.5%) systems (Table 1). Furthermore, a prominent effect for the photocurrent generation was also observed for (ZnP-ester + C₆₀-acid)/SnO₂/ITO (7.1%) in comparison with those of (ZnP-ester + C₆₀-ester)/SnO₂/ITO (2.6%) and ZnP-ester/SnO₂/ITO (1.2%) systems. The increase may be attributed to the enhancement of hydrogen bonding between C₆₀-acid molecules in the mixed film, as shown in Figure 3g. These results demonstrate that photocurrent generation is much enhanced in a hydrogen-bonded porphyrin–fullerene system compared with the reference system without hydrogen bonding.

Photophysical Studies. At first, steady-state fluorescence spectra ($\lambda_{\text{ex}} = 430 \text{ nm}$) were measured for the better understanding of the photodynamical behavior of the porphyrin–fullerene system on the SnO₂ electrodes prepared by the dipping method (Figure 7). Fluorescence from the porphyrin is strongly quenched in (ZnP-acid + C₆₀-acid)/SnO₂/ITO and (ZnP-acid + C₆₀-ester)/SnO₂/ITO relative to ZnP-acid/SnO₂/ITO. In the ZnP-acid system, no emission from the C₆₀ moiety (720 nm) is seen except the case of (ZnP-acid + C₆₀-acid)/SnO₂/ITO⁴⁰ (Figure 7a). The intensity of the fluorescence due to the porphyrin moiety in the ZnP-acid system is in the order of (ZnP-acid + C₆₀-acid)/SnO₂/ITO < (ZnP-acid + C₆₀-ester)/SnO₂/ITO < ZnP-acid/SnO₂/ITO, which is consistent with that of the IPCE values. Similar porphyrin fluorescence quenching was observed for (ZnP-ester + C₆₀-acid)/SnO₂/ITO and (ZnP-ester + C₆₀-ester)/SnO₂/ITO in comparison with ZnP-ester/SnO₂/ITO (Figure 7b). These results suggest the occurrence of photoinduced electron transfer or partial charge transfer (i.e., exciplex formation) from the porphyrin excited singlet state to the C₆₀ moiety (vide infra).²⁹ It is noteworthy that (ZnP-ester + C₆₀-acid)/SnO₂/ITO reveals the emission from both the porphyrin

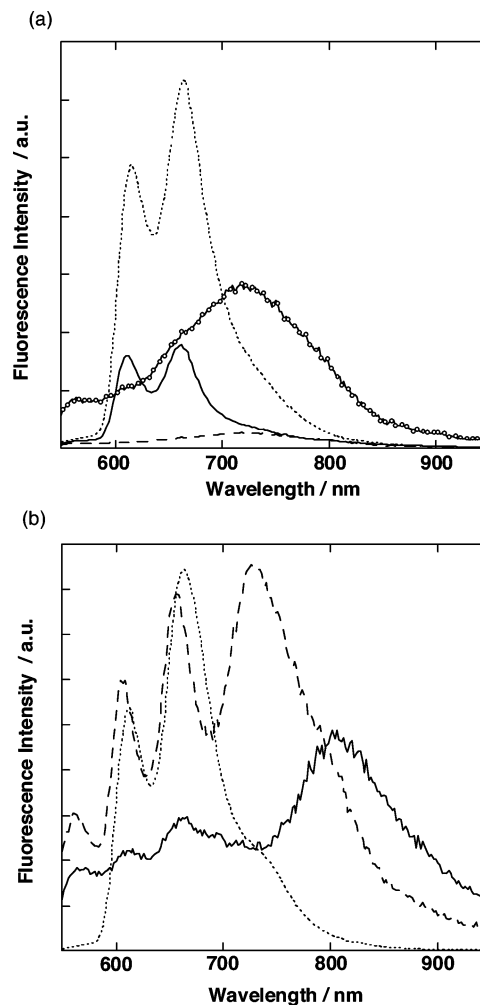


Figure 7. Steady-state fluorescence spectra of (a) ZnP-acid/SnO₂/ITO (dotted line), (ZnP-acid + C₆₀-ester)/SnO₂/ITO (solid line, [ZnP]/[C₆₀] = 1:1), and (ZnP-acid + C₆₀-acid)/SnO₂/ITO (dashed line and solid line with white circles ($\times 10$); [ZnP]/[C₆₀] = 1:1) electrodes. (b) ZnP-ester/SnO₂/ITO (dotted line ($\times 10^{-2}$)), (ZnP-ester + C₆₀-ester)/SnO₂/ITO (solid line, [ZnP]/[C₆₀] = 1:1), and (ZnP-ester + C₆₀-acid)/SnO₂/ITO (dashed line, [ZnP]/[C₆₀] = 1:1) electrodes. The excitation wavelength was 430 nm.

and the C₆₀ moieties,⁴⁰ which agrees with the results on the IRRA spectrum (Figure 3g). On the other hand, (ZnP-ester + C₆₀-ester)/SnO₂/ITO exhibit CT emission (800 nm),²⁵ in addition to the weak emission from the porphyrin. In the case of (ZnP-ester + C₆₀-ester)/SnO₂/ITO, ZnP-ester and C₆₀-ester molecules are susceptible to make close contact due to the π - π interaction because of the absence of hydrogen bonding. Accordingly, most of the ZnP-ester and C₆₀-ester make the supramolecular complex to exhibit CT emission, whereas the minor, uncomplex ZnP-ester and C₆₀-ester reveals the quenching of fluorescence from the porphyrin moiety via photoinduced ET (vide infra).

Photoinduced electron-transfer process was confirmed by the comparison of picosecond fluorescence lifetime measurements for (ZnP-acid + C₆₀-acid)/SnO₂/ITO, (ZnP-acid + C₆₀-ester)/SnO₂/ITO, (ZnP-ester + C₆₀-acid)/SnO₂/ITO, (ZnP-ester + C₆₀-ester)/SnO₂/ITO, ZnP-acid/SnO₂/ITO, and ZnP-ester/SnO₂/ITO systems prepared by the dipping method. The fluorescence lifetimes on the SnO₂/ITO surfaces were measured by a time-correlated single-photon counting technique at emission wavelength of 660 nm due to the porphyrin moiety with excitation at 590 nm. The decay curves of the fluorescence intensity were fitted by three exponentials (Figure 8). However, in all cases, the fastest component was the dominating one (>80%). The

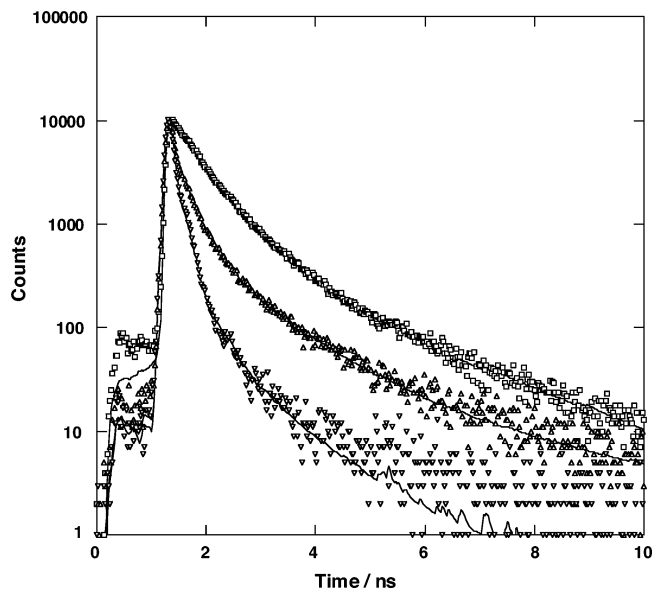


Figure 8. Fluorescence decay curves of (a) ZnP-ester/SnO₂/ITO (square), (b) (ZnP-ester + C₆₀-ester)/SnO₂/ITO (upper triangle, [ZnP]/[C₆₀] = 1:1), and (c) (ZnP-ester + C₆₀-acid)/SnO₂/ITO (downward triangle, [ZnP]/[C₆₀] = 1:1) electrodes observed at 660 nm by the single photon counting method. The excitation wavelength is 590 nm.

lifetimes of the fastest component are summarized in Table 1. The fluorescence lifetimes of (ZnP-acid + C₆₀-acid)/SnO₂/ITO, (ZnP-acid + C₆₀-ester)/SnO₂/ITO, and ZnP-acid/SnO₂/ITO are much shorter than the time resolution of the present system (<40 ps).⁴¹ This is in accordance with the stepwise electron transfer from the porphyrin excited singlet state to the C₆₀, followed by electron injection to the CB of the SnO₂ electrode, in addition to the fast, direct electron injection of the porphyrin singlet excited state to the CB of the SnO₂ electrode through the chemical adsorption of carboxylic acid group onto the SnO₂ surface.^{36,37} The fluorescence lifetimes of (ZnP-ester + C₆₀-acid)/SnO₂/ITO (40 ps) and (ZnP-ester + C₆₀-ester)/SnO₂/ITO (62 ps) are shorter than that of ZnP-ester/ITO systems (380 ps), where direct electron injection process from the porphyrin excited singlet state to the CB of the SnO₂ electrode is suppressed due to the absence of chemical adsorption of the porphyrin onto the SnO₂ surface. These results support the occurrence of photoinduced electron transfer or partial charge transfer from the porphyrin singlet excited state to the C₆₀ moiety rather than self-quenching of the porphyrin excited state due to the aggregation to yield the charge-separated state, which eventually leads to the photocurrent generation.

The formation of the charge-separated state in the mixed films was detected using the femtosecond pump-probe method for (ZnP-ester + C₆₀-ester)/SnO₂/ITO, ZnP-acid/SnO₂/ITO, and ZnP-ester/SnO₂/ITO systems with the excitation wavelength of 555 nm. The transient absorption spectrum of (ZnP-ester + C₆₀-ester)/SnO₂/ITO, prepared by dipping method, reveals the characteristic bands around 650 nm due to zinc porphyrin radical cation²⁵ and 1000 nm due to C₆₀ radical anion²⁵ (Figure 9), which thus can be assigned to the charge-separated state or to the exciplex state.^{21,25,29} With the time resolution of the instrument used an instant formation of the bands was observed, which indicates that the primary exciplex formation in the sample can be as fast as 10¹³ s⁻¹. This is consistent with the observation of CT emission due to the π -complexation between the porphyrin and the C₆₀ in the steady-state fluorescence spectrum of (ZnP-ester + C₆₀-ester)/SnO₂/ITO. The decay of the transient absorption was a complex process with the fastest relaxation rate of 10¹¹ s⁻¹, which was followed by a slower

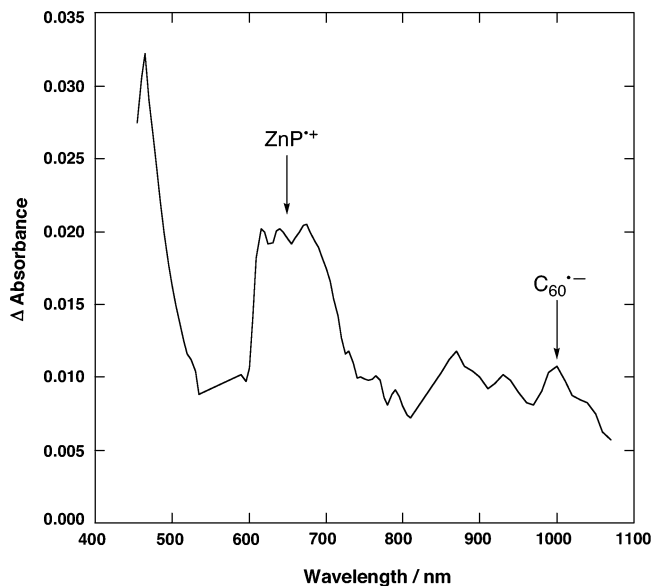
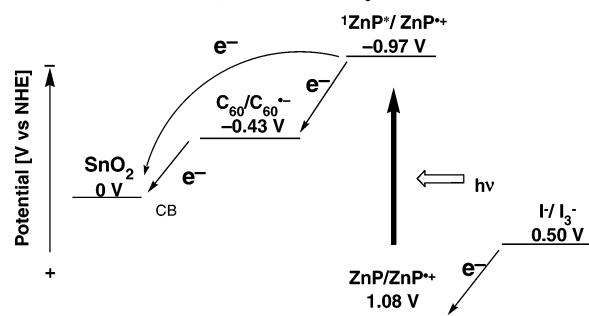


Figure 9. Transient absorption spectrum of (ZnP-ester + C₆₀-ester)/SnO₂/ITO at a time delay of 10 ps excited at 555 nm.

SCHEME 2: Photocurrent Generation Diagram for the (ZnP-acid + C₆₀-acid)/SnO₂/ITO System



relaxation with the rate constant even smaller than 10⁹ s⁻¹. This can be understood in terms of different types of structures formed and a variety of charge-separation pathways realized in the system. In contrast, the transient absorption spectra of ZnP-acid/SnO₂/ITO and ZnP-ester/SnO₂/ITO exhibit the characteristic bleaching around 590 nm due to the porphyrin excited singlet state.^{21,25,29,42}

Based on the energetics of the photoactive and radical ion species involved in (ZnP-acid + C₆₀-acid)/SnO₂/ITO system, the mechanism of anodic photocurrent generation is proposed (Scheme 2). First, an electron transfer takes place from ¹ZnP* (ZnP-acid, 0.97 V; ZnP-ester, 0.96 V (vs NHE)) to the conduction band of SnO₂ (0 V vs NHE)²⁰ or C₆₀ (C₆₀-acid, -0.43 V; C₆₀-ester, 0.32 V (vs NHE)),²⁰ yielding the porphyrin radical cation (ZnP•⁺) and the electron in the conduction band or ZnP•⁺ and C₆₀ radical anion (C₆₀•⁻).⁴³ In the latter case, the reduced C₆₀•⁻ gives an electron to the conduction band of SnO₂ (0 V vs SCE)²⁰ to yield the same state. On the other hand, I⁻ (0.5 V vs NHE)²⁰ donates an electron to ZnP•⁺ (ZnP-acid, 1.08 V; ZnP-ester, 1.09 V (vs NHE))²⁰ to generate anodic photocurrent. The hydrogen bonding in the porphyrin or the C₆₀ molecules or both may be responsible for the large IPCE values in comparison with the reference system without the hydrogen bonding. Such hydrogen bonding would facilitate the initial charge separation between the porphyrin and the C₆₀ and the separated electron and hole relay through the hydrogen-bonded arrays which suppress the undesirable charge recombination. It is well-known that the use of acid functionalized dyes helps in

adsorbing the dye to the metal oxide.¹² The advantage of this approach compared to such conventional dye-sensitized solar cells is the acid groups can contribute both binding to SnO₂ and binding the molecules to one another. Although the present system is rather complex relative to the dye-sensitized solar cells, such binding properties would be modulated by varying the chemical modification conditions (i.e., spin-coating, dipping, and electrophoretic deposition methods) to optimize the photoelectrochemical properties.

Conclusion

Hydrogen bonding effects on photocurrent generation have been examined in the mixed films of porphyrin and/or fullerene with and without hydrogen bonding on nanostructured SnO₂ electrodes. The nanostructured SnO₂ electrodes modified with the mixed films of porphyrin and fullerene with hydrogen bonding exhibit efficient photocurrent generation (up to IPCE value of 36%) as compared to the reference systems without hydrogen bonding. Atomic force microscopy, infrared reflection absorption and ultraviolet-visible absorption spectroscopies, and time-resolved fluorescence lifetime and transient absorption measurements support the significant contribution of hydrogen-bonding interaction between the porphyrins or the C₆₀ moieties or the both in the films on the electrode surface for the photocurrent generation efficiency. These results show that hydrogen bonding is a highly promising methodology for the construction of molecular photoelectrochemical devices.

Acknowledgment. This work was supported by the Integrative Industry-Academia Partnership (IIAP) including Kyoto University, Nippon Telegraph and Telephone Corp., Pioneer Corp., Hitachi, Ltd., Mitsubishi Chemical Corp., and Rohm Co., Ltd. H.I. also thanks Grant-in-Aid from MEXT, Japan (No. 16310073 and 21st Century COE on Kyoto University Alliance for Chemistry) for financial support. S.Y. acknowledges support from Nippon Sheet Glass Foundation for Materials Science and Engineering. M.I., N.V.T., and H.L. thank the Academy of Finland for the financial support.

Supporting Information Available: Section profiles of AFM images (S1). This material is available free of charge via the Internet at <http://pubs.acs.org>.

References and Notes

- (1) (a) *The Photosynthetic Reaction Center*; Deisenhofer, J., Norris, J. R., Eds.; Academic Press: San Diego, 1993. (b) *Anoxygenic Photosynthetic Bacteria*; Blankenship, R. E., Madigan, M. T., Bauer, C. E., Eds.; Kluwer: Dordrecht, The Netherlands, 1995.
- (2) (a) Lehn, J.-M. *Supramolecular Chemistry: Concepts and Perspectives*; VCH: Weinheim, Germany, 1995. (b) Sessler, J. L.; Wang, B.; Springs, S. L.; Brown, C. T. In *Comprehensive Supramolecular Chemistry*; Atwood, J. L., Davies, J. E. D., Eds.; Pergamon: New York, 1996. (c) Chang, C. J.; Brown, J. D. K.; Chang, M. C. Y.; Baker, E. A.; Nocera, D. G. In *Electron Transfer in Chemistry*; Balzani, V., Ed.; Wiley-VCH: Weinheim, Germany, 2001; Vol. 2, pp 408–461. (d) *Molecular Catenanes, Rotaxanes and Knots*, Sauvage, J.-P., Dietrich-Buchecker, C., Eds.; Wiley-VCH: Weinheim, Germany, 1999.
- (3) (a) Hunter, C. A.; Sanders, J. K. M.; Beddard, G. S.; Evans, S. *Chem. Commun.* **1989**, 1765. (b) Anderson, H. L.; Hunter, C. A.; Sanders, J. K. M. *J. Chem. Soc., Chem. Commun.* **1989**, 226. (c) McClenaghan, N. D.; Grote, Z.; Darriet, K.; Zimine, M.; Williams, R. M.; De Cola, L.; Bassani, D. M. *Org. Lett.* **2005**, *7*, 807. (d) Smitha, M. A.; Prasad, E.; Gopidas, K. R. *J. Am. Chem. Soc.* **2001**, *123*, 1159. (e) Prasad, E.; Gopidas, K. R. *J. Am. Chem. Soc.* **2000**, *122*, 3191.
- (4) (a) de Rege, P. J. F.; Williams, S. A.; Therien, M. J. *Science* **1995**, *269*, 1409. (b) Harriman, A.; Magda, D. J.; Sessler, J. L. *Chem. Commun.* **1991**, 345. (c) Sessler, J. L.; Wang, B.; Harriman, A. *J. Am. Chem. Soc.* **1995**, *117*, 704. (d) Berman, A.; Izraeli, E. S.; Levanon, H.; Wang, B.; Sessler, J. L. *J. Am. Chem. Soc.* **1995**, *117*, 8252.
- (5) (a) Hayashi, T.; Ogoshi, H. *Chem. Soc. Rev.* **1997**, *26*, 355. (b) Blanco, M.-J.; Jiménez, M. C.; Chambron, J.-C.; Heitz, V.; Linke, M.; Sauvage, J.-P. *Chem. Soc. Rev.* **1999**, *28*, 293. (c) Willner, I.; Kaganer, E.; Joselevich, E.; Dürr, H.; David, E.; Günter, M. J.; Johnston, M. R. *Coord. Chem. Rev.* **1998**, *171*, 261. (d) Jensen, H.; Kakkassery, J. J.; Nagatani, H.; Fermin, D. J.; Girault, H. H. *J. Am. Chem. Soc.* **2000**, *122*, 10943.
- (6) (a) D'Souza, F.; Rath, N. P.; Deviprasad, G. R.; Zandler, M. E. *Chem. Commun.* **2001**, 267. (b) D'Souza, F.; Deviprasad, G. R.; El-Khouly, M. E.; Fujitsuka, M.; Ito, O. *J. Am. Chem. Soc.* **2001**, *123*, 5277. (c) D'Souza, F.; Deviprasad, G. R.; Rahman, M. S.; Choi, J. *Inorg. Chem.* **1999**, *38*, 2157. (d) D'Souza, F.; Zandler, M. E.; Smith, P. M.; Deviprasad, G. R.; Arkady, K.; Fujitsuka, M.; Ito, O. *J. Phys. Chem. A* **2002**, *106*, 649. (e) D'Souza, F.; Deviprasad, G. R.; Zandler, M. E.; El-Khouly, M. E.; Fujitsuka, M.; Ito, O. *J. Phys. Chem. A* **2003**, *107*, 4801. (f) D'Souza, F.; Smith, P. M.; Zandler, M. E.; McCarty, A. L.; Ito, M.; Araki, Y.; Ito, O. *J. Am. Chem. Soc.* **2004**, *126*, 7898.
- (7) (a) Otsuki, J.; Harada, K.; Toyama, K.; Hirose, Y.; Araki, K.; Seno, M.; Takatera, K.; Watanabe, T. *Chem. Commun.* **1998**, 1515. (b) Imahori, H.; Yoshizawa, E.; Yamada, K.; Hagiwara, K.; Okada, T.; Sakata, Y. *Chem. Commun.* **1995**, 1133. (c) Imahori, H.; Yamada, K.; Yoshizawa, E.; Hagiwara, K.; Okada, T.; Sakata, Y. *J. Porphyrins Phthalocyanines* **1997**, *1*, 55. (d) Yamada, K.; Imahori, H.; Yoshizawa, E.; Gosztola, D.; Wasielewski, M. R.; Sakata, Y. *Chem. Lett.* **1999**, 235.
- (8) (a) Da Ros, T.; Prato, M.; Guldi, D. M.; Ruzzi, M.; Pasimeni, L. *Chem. Eur. J.* **2001**, *7*, 816. (b) Armaroli, N.; Diederich, F.; Echegoyen, L.; Habicher, T.; Flamigni, L.; Marconi, G.; Nierengarten, J.-F. *New. J. Chem.* **1999**, *77*. (c) D'Souza, F. *J. Am. Chem. Soc.* **1996**, *118*, 923.
- (9) (a) Guldi, D. M.; Martín, N. *J. Mater. Chem.* **2002**, *12*, 1978. (b) Segura, M.; Sanchez, L.; de Mendoza, J.; Martín, N.; Guldi, D. M. *J. Am. Chem. Soc.* **2003**, *125*, 15093. (c) Fang, H.; Wang, S.; Xiao, S.; Yang, J.; Liu, Y.; Shi, Z.; Li, H.; Liu, H.; Xiao, S.; Zhu, D. *Chem. Mater.* **2003**, *15*, 1593.
- (10) (a) Beckers, E. H. A.; Schenning, A. P. H. J.; van Hal, P. A.; El-ghayoury, A.; Sanchez, L.; Hummelen, J. C.; Meijer, E. W.; Janssen, R. A. *J. Chem. Commun.* **2002**, 2888. (b) Beckers, E. H. A.; van Hal, P. A.; Schenning, A. P. H. J.; El-ghayoury, A.; Peeters, E.; Rispens, M. T.; Hummelen, J. C.; Meijer, E. W.; Janssen, R. A. *J. Mater. Chem.* **2002**, *2054*. (c) Neuteboom, E. E.; Beckers, E. H. A.; Meskers, S. C. J.; Meijer, E. W.; Janssen, R. A. *J. Org. Biomol. Chem.* **2003**, *1*, 198.
- (11) (a) Li, K.; Schuster, D. I.; Guldi, D. M.; Herranz, M. A.; Echegoyen, L. *J. Am. Chem. Soc.* **2004**, *126*, 3388. (b) Li, K.; Bracher, P. J.; Guldi, D. M.; Herranz, M. A.; Echegoyen, L.; Schuster, D. I. *J. Am. Chem. Soc.* **2004**, *126*, 9156.
- (12) (a) Hagfeldt, A.; Grätzel, M. *Acc. Chem. Res.* **2000**, *33*, 269. (b) Grätzel, M. *Nature* **2001**, *414*, 338. (c) Bignozzi, C. A.; Argazzi, R.; Kleverlaan, C. *J. Chem. Soc. Rev.* **2000**, *29*, 87.
- (13) (a) Yu, G.; Gao, J.; Hummelen, J. C.; Wudl, F.; Heeger, A. J. *Science* **1995**, *270*, 1789. (b) Wudl, F. *J. Mater. Chem.* **2002**, *12*, 1959.
- (14) (a) Shaheen, S. E.; Brabec, C. J.; Sariciftci, N. S.; Padinger, F.; Fromherz, T.; Hummelen, J. C. *Appl. Phys. Lett.* **2001**, *78*, 841. (b) Padinger, F.; Rittberger, R. S.; Sariciftci, N. S. *Adv. Funct. Mater.* **2003**, *13*, 85.
- (15) (a) Schmidt-Mende, L.; Fechtenkötter, A.; Müllen, K.; Moons, E.; Friend, R. H.; MacKenzie, J. D. *Science* **2001**, *293*, 1119. (b) Halls, J. J. M.; Walsh, C. A.; Greenham, N. C.; Marseglia, E. A.; Friend, R. H.; Moratti, S. C.; Holmes, A. B. *Nature* **1995**, *376*, 498. (c) Granström, M.; Petritsch, K.; Arias, A. C.; Lux, A.; Andersson, M. R.; Friend, R. H. *Nature* **1998**, *395*, 257. (d) Huynh, W. U.; Dittmer, J. J.; Alivisatos, A. P. *Science* **2002**, *295*, 2425. (e) Liu, J.; Tanaka, T.; Sivula, K.; Alivisatos, A. P.; Fréchet, J. M. J. *J. Am. Chem. Soc.* **2004**, *126*, 6550.
- (16) (a) Tsuzuki, T.; Shirota, Y.; Rostalski, J.; Meissner, D. *Solar Energy Mater. Solar Cells* **2000**, *61*, 1. (b) Xue, J.; Rand, B. P.; Uchida, S.; Forrest, S. R. *Adv. Mater.* **2005**, *17*, 66.
- (17) (a) Wienk, M. M.; Kroon, J. M.; Verhees, W. J. H.; Knol, J.; Hummelen, J. C.; van Hal, P. A.; Janssen, R. A. *J. Angew. Chem., Int. Ed.* **2003**, *42*, 3371. (b) Dhanabalan, A.; van Duren, J. K. J.; van Hal, P. A.; van Dongen, J. L. J.; Janssen, R. A. *J. Adv. Funct. Mater.* **2001**, *11*, 255.
- (18) (a) Eckert, J.-F.; Nicoud, J.-F.; Nierengarten, J.-F.; Liu, S.-G.; Echegoyen, L.; Barigelletti, F.; Armaroli, N.; Ouali, L.; Krasnikov, V.; Hadziioannou, G. *J. Am. Chem. Soc.* **2000**, *122*, 7467. (b) Lahav, M.; Heleg-Shabtai, V.; Wasserman, J.; Katz, E.; Willner, I.; Dürr, H.; Hu, Y.-Z.; Bossmann, S. H. *J. Am. Chem. Soc.* **2000**, *122*, 11480.
- (19) (a) Liu, Y.; Xiao, S.; Li, H.; Li, Y.; Liu, H.; Lu, F.; Zhuang, J.; Zhu, D. *J. Phys. Chem. B* **2004**, *108*, 6256. (b) Imahori, H.; Liu, J.-C.; Hosomizu, K.; Sato, T.; Mori, Y.; Hotta, H.; Matano, Y.; Araki, Y.; Ito, O.; Maruyama, N.; Fujita, S. *Chem. Commun.* **2004**, 2066.
- (20) (a) Hasobe, T.; Imahori, H.; Fukuzumi, S.; Kamat, P. V. *J. Phys. Chem. B* **2003**, *107*, 12105. (b) Hasobe, T.; Kashiwagi, Y.; Absalom, M. A.; Sly, J.; Hosomizu, K.; Crossley, M. J.; Imahori, H.; Kamat, P. V.; Fukuzumi, S. *Adv. Mater.* **2004**, *16*, 975. (c) Hasobe, T.; Imahori, H.; Kamat, P. V.; Fukuzumi, S. *J. Am. Chem. Soc.* **2003**, *125*, 14962. (d) Imahori, H. *J. Phys. Chem. B* **2004**, *108*, 6130. (e) Imahori, H.; Fukuzumi, S. *Adv. Funct. Mater.* **2004**, *14*, 525.

- (21) (a) Imahori, H.; Sakata, Y. *Adv. Mater.* **1997**, *9*, 537. (b) Imahori, H.; Sakata, Y. *Eur. J. Org. Chem.* **1999**, *2445*, 5. (c) Imahori, H.; Mori, Y.; Matano, Y. *J. Photochem. Photobiol. C* **2003**, *4*, 51. (d) Imahori, H. *Org. Biomol. Chem.* **2004**, *2*, 1425.
- (22) (a) Fukuzumi, S.; Guldi, D. M. In *Electron Transfer in Chemistry*; Balzani, V., Ed.; Wiley-VCH: Weinheim, Germany, 2001; Vol. 2, pp 270–337. (b) Guldi, D. M.; Prato, M. *Acc. Chem. Res.* **2000**, *33*, 695. (c) Gust, D.; Moore, T. A.; Moore, A. L. *Acc. Chem. Res.* **2001**, *34*, 40.
- (23) (a) Evans, D. R.; Fackler, N. L. P.; Xie, Z.; Rickard, C. E. F.; Boyd, P. D. W.; Reed, C. A. *J. Am. Chem. Soc.* **1999**, *121*, 8466. (b) Sun, D.; Tham, F. S.; Reed, C. A.; Chaker, L.; Boyd, P. D. W. *J. Am. Chem. Soc.* **2002**, *124*, 6604. (c) Tashiro, K.; Aida, T.; Zheng, J.-Y.; Kinbara, K.; Saigo, K.; Sakamoto, S.; Yamaguchi, K. *J. Am. Chem. Soc.* **1999**, *121*, 9477.
- (24) (a) Yamaguchi, T.; Ishii, N.; Tashiro, K.; Aida, T. *J. Am. Chem. Soc.* **2003**, *125*, 13934. (b) Kimura, M.; Saito, Y.; Ohta, K.; Hanabusa, K.; Shirai, H.; Kabayashi, N. *J. Am. Chem. Soc.* **2002**, *124*, 5274. (c) Shirakawa, M.; Fujita, N.; Shinkai, S. *J. Am. Chem. Soc.* **2003**, *125*, 9902.
- (25) (a) Imahori, H.; Hagiwara, K.; Aoki, M.; Akiyama, T.; Taniguchi, S.; Okada, T.; Shirakawa, M.; Sakata, Y. *J. Am. Chem. Soc.* **1996**, *118*, 11771. (b) Imahori, H.; Tkachenko, N. V.; Vehmanen, V.; Tamaki, K.; Lemmetyinen, H.; Sakata, Y.; Fukuzumi, S. *J. Phys. Chem. A* **2001**, *105*, 1750. (c) Tkachenko, N. V.; Guenther, C.; Imahori, H.; Tamaki, K.; Sakata, Y.; Fukuzumi, S.; Lemmetyinen, H. *Chem. Phys. Lett.* **2000**, *326*, 344. (d) Vehmanen, V.; Tkachenko, N. V.; Imahori, H.; Fukuzumi, S.; Lemmetyinen, H. *Spectrochim. Acta, Part A* **2001**, *57*, 2229. (e) Guldi, D. M.; Luo, C.; Prato, M.; Troisi, A.; Zerbetto, F.; Scheloske, M.; Diel, E.; Bauer, W.; Hirsch, A. *J. Am. Chem. Soc.* **2001**, *123*, 9166.
- (26) Li, G.; Morita, S.; Ye, S.; Tanaka, M.; Osawa, M. *Anal. Chem.* **2004**, *76*, 788.
- (27) Nierengarten, J.-F.; Eckert, J.-F.; Rio, Y.; del Pilar Carreon, M. P.; Gallani, J.-L.; Guillon, D. *J. Am. Chem. Soc.* **2001**, *123*, 9743.
- (28) Luo, C.; Guldi, D. M.; Imahori, H.; Tamaki, K.; Sakata, Y. *J. Am. Chem. Soc.* **2000**, *122*, 6535.
- (29) (a) Tkachenko, N. V.; Rantala, L.; Tauber, A. Y.; Helaja, J.; Hynninen, P. H.; Lemmetyinen, H. *J. Am. Chem. Soc.* **1999**, *121*, 9378. (b) Kesti, T. J.; Tkachenko, N. V.; Vehmanen, V.; Yamada, H.; Imahori, H.; Fukuzumi, S.; Lemmetyinen, H. *J. Am. Chem. Soc.* **2002**, *124*, 8067. (c) Tkachenko, N. V.; Lemmetyinen, H.; Sonoda, J.; Ohkubo, K.; Sato, T.; Imahori, H.; Fukuzumi, S. *J. Phys. Chem. A* **2003**, *107*, 8834.
- (30) (a) Pasimeni, L.; Hirsch, A.; Lamparth, I.; Maggini, M.; Prato, M. *J. Am. Chem. Soc.* **1997**, *119*, 12902. (b) Camps, X.; Hirsch, A. *J. Chem. Soc., Perkin Trans. 1* **1997**, 1595.
- (31) Colthup, N. B.; Daly, L. H.; Wiberley, S. E. *Introduction to Infrared and Raman Spectroscopy*, 3rd ed.; Academic Press: San Diego, CA, 1990.
- (32) Génin, F.; Quilès, F.; Burneau, A. *Phys. Chem. Chem. Phys.* **2001**, *3*, 932.
- (33) Dong, J.; Ozaki, Y. *Macromolecules* **1997**, *30*, 286.
- (34) Ye, S.; Morita, S.; Li, G.; Noda, H.; Tanaka, M.; Uosaki, K.; Osawa, M. *Macromolecules* **2003**, *36*, 5694.
- (35) Li, G.; Ye, S.; Morita, S.; Nishida, T.; Osawa, M. *J. Am. Chem. Soc.* **2004**, *126*, 12198.
- (36) (a) Durrant, J. R.; Haque, S. A.; Palomares, E. *Coord. Chem. Rev.* **2004**, *248*, 1247. (b) Gregg, B. A. *Coord. Chem. Rev.* **2004**, *248*, 1215. (c) Katoh, R.; Furube, A.; Barzykin, A. V.; Arakawa, H.; Tachiya, M. *Coord. Chem. Rev.* **2004**, *248*, 1195. (d) Tachibana, Y.; Moser, J. E.; Grätzel, M.; Klug, D. R.; Durrant, J. R. *J. Phys. Chem.* **1996**, *100*, 20056. (e) Kay, A.; Humphry-Baker, R.; Grätzel, M. *J. Phys. Chem.* **1994**, *98*, 952. (f) Clifford, J. N.; Palomares, E.; Nazeeruddin, M. K.; Grätzel, M.; Nelson, J.; Li, X.; Long, N. J.; Durrant, J. R. *J. Am. Chem. Soc.* **2004**, *126*, 5225.
- (37) (a) Ellingson, R. J.; Asbury, J. B.; Ferrere, S.; Ghosh, H. N.; Sprague, J. R.; Lian, T. Q.; Nozik, A. J. *J. Phys. Chem. B* **1998**, *102*, 6455. (b) Fessenden, R. W.; Kamat, P. V. *J. Phys. Chem.* **1995**, *99*, 12902. (c) Asbury, J. B.; Hao, E.; Wang, Y. Q.; Ghosh, H. N.; Lian, T. Q. *J. Phys. Chem. B* **2001**, *105*, 4545. (d) Watson, D. F.; Marton, A.; Stux, A. M.; Meyer, G. J. *J. Phys. Chem. B* **2004**, *108*, 11680. (e) Wienke, J.; Schaafsma, T. J.; Goossens, A. *J. Phys. Chem. B* **1999**, *103*, 2702. (f) Koehorst, R. B. M.; Boschloo, G. K.; Savenije, T. J.; Goossens, A.; Schaafsma, T. J. *J. Phys. Chem. B* **2000**, *104*, 2371. (g) Fungo, F.; Otero, L.; Durantini, E. N.; Silber, J. J.; Sereno, L. E. *J. Phys. Chem. B* **2000**, *104*, 7644.
- (38) We also examined the effect of the relative ratios of ZnP-acid and C₆₀-acid on the IPCE values under the same experimental conditions. The largest IPCE value (36%) was obtained when a mixed solution with the relative ratio of [ZnP-acid]:[C₆₀-acid] = 1:1 was employed for the preparation of the modified SnO₂ electrode.
- (39) Thickness of the SnO₂ layer (0.1–1.1 μm) on the ITO electrode was also varied to optimize the IPCE value. The largest IPCE value (36%) was achieved when the thickness of the SnO₂ layer was 1.1 μm. Further increase of the thickness of the SnO₂ layer resulted in the formation of extremely rough SnO₂ layer.
- (40) The weak emission from the C₆₀ moiety (C₆₀-acid) may be attributed to the direct excitation of the C₆₀ moiety in which some part of the identical C₆₀-acid molecules form hydrogen-bonded aggregates without making a supramolecular complex with the zinc porphyrin, as suggested from the IRRA spectra.
- (41) We also tried to measure the fluorescence lifetimes on SnO₂ electrodes using an up-conversion method (time resolution, ~100 fs), but it was not possible because the excitation light destroys the sample at the excitation spot very quickly.
- (42) A reliable conclusion could not be drawn from the transient absorption spectra of (ZnP-acid + C₆₀-acid)/SnO₂/ITO, (ZnP-ester + C₆₀-ester)/SnO₂/ITO, and (ZnP-ester + C₆₀-acid)/SnO₂/ITO systems because of the weak signals and the degradation of the samples under laser irradiation.
- (43) The first reduction and oxidation potentials were determined by using cyclic voltammetric measurements in THF containing 0.1 M Bu₄-NPF₆. The energy level of the porphyrin excited singlet state was estimated to be 2.05 eV in THF from the absorption and emission spectra.